Revista Argentina de Clínica Psicológica
2021, Vol. XXX, N°1, 269-282
DOI: 10.24205/03276716.2020.2023

Using artificial intelligence to determine the patient infection time with Coronavirus and report the level of medical care needed

Ashraf Elfasakhany*, Mishal Alsehli, Farhan A. Salem

Abstract
The Coronavirus has rapidly spread and reached more than 200 countries, infecting several million worldwide in a few weeks. Artificial intelligence (AI) techniques have been proven useful in testing, diagnosing, and effectively reducing the spread of the virus. However, some problems or deficiencies are found in the current AI techniques. Patients are diagnosed after the emergence of symptoms; thus, deciding the necessary patient care is difficult. The intervention of doctors is compulsory, thus leading to possible infection with the virus due to direct contact with patients. The current work aims to develop AI techniques to overcome such problems. This study proposes AI capable of determining the infection time of patients with the virus and the level of medical care needed before the onset of COVID-19 symptoms. The proposed device measures many vital biological and human functions, such as the state of the brain and neurotransmitters, mental/mood conditions, tension level of face muscles, hands and body temperature, rate of pulse and pressure, oxygen level in the blood, rate of breathing and its difficulty, degree of redness of eye(s), and general body imbalances. Hardware and software designs are applied in this work. An experimental study is applied to examine, test, and evaluate the integration/work of each subsystem component and the overall system design. Results showed that the proposed system, could be used to distinguish between healthy and infected individuals before the onset of COVID-19 symptoms.
Keywords: Artificial intelligence; Coronavirus; diagnosis; time of infection; level of medical care needed.

1. Introduction

The coronavirus is one of the most widespread diseases according to the World Health Organization, indicating that the virus has reached more than 200 countries worldwide and an infection rate of more than 81 million people thus far. Many governments and health organizations are scrambling to control the spread of the novel coronavirus disease pneumonia (COVID-19). Artificial intelligence (AI) techniques are shown to be one of the most effective methods, which have been proven useful in tracking the spread of the virus, diagnosing patients, clearing areas, and speeding up the process of finding an effective vaccine and other things that can help eradicate this epidemic.

Covid-19, a slightly new disease, is a virus that emerged for the first time in the city of Wuhan, China, in December 2019 [1–4]. In January 2020, the clinical characteristics of 41 patients were summarized with COVID-19 by Huang et al. [5]. Subsequently, AI is considered to help for controlling COVID-19. Researchers concluded that the use of AI is one of the most important reasons that have helped China in limiting the spread of the virus in record time. The background of the discovery of the disease and its confirmation through AI relies on tracking the spread of infectious diseases worldwide. Such a discovery announced the existence of a group of unusual pneumonia cases that occurred at a market in Wuhan, China. AI also tracked global airline ticket data for predicting the path and timing of travel for the infected population thereafter. Thus, AI proved to be a powerful tool for the appointed prediction of COVID-19 [6,7].

AI may integrate with image analysis technique to provide one of the tools for detection,

Mechanical Engineering Department, College of Engineering, Taif University, P.O. Box 11099, Taif 21944, Saudi Arabia.
Correspondence: ashr12000@yahoo.com; a.taha@tu.edu.sa; Tel.: +966 (02) 7272020; Fax: +966 (02)7274299

quantification, AI, and monitoring of coronavirus [8]. The technologies for digital image processing have been considered promising in coronavirus diagnosis [9,10]. In addition to the powerful facility of non-linear modeling, medical image processing using general neural networks was conducted in the diagnosis and calculation of the infection possibility of COVID-19 [11–14]. Shan et al. [15] developed a deep learning-based system for automatic segmentation of lungs and infection sites using chest CT scan. Xu et al. [16] investigated a screening model for differentiating between influenza and COVID-19 for viral pneumonia using pulmonary CT images and deep learning techniques. Wang et al. [17] developed a deep learning method based on the graphical features of COVID-19 to provide a clinical diagnosis before pathogenic testing. Hamimi et al. [18] showed that COVID-19 has particular radiological signatures and image patterns as observed in CT scans. Szegedy et al. [19] examined neural networks to distinguish between infected and non-infected person(s) with COVID-19. The dataset highlights 259 patients using thousands of images to emphasize the model for COVID-19. Similarly, Zhou et al. [20] and Chen et al. [21] applied neural networks using between 5000 and 6000 images on different people (healthy and unhealthy) to introduce the diagnostic attitude of COVID-19. Wang [22] proposed a deep conventional neural network called COVID-Net for the detection of COVID-19 cases from chest X-ray images with 83.5% accuracy. Wang et al. [23] used deep learning techniques on CT images to screen COVID-19 patients with 89% accuracy. Joaquin [24] utilized a small dataset of 339 images for training and testing deep learning technique and reported a validation technique with 96.2% accuracy. The study presented a model to classify COVID-19 and normal X-ray images. Yan et al. [25] built a predictive model to identify early detection of high-risk patients before the transition from mild to critical symptoms. Santosh [26] focused on the design of new paradigms based on AI-driven tools using a combination of machine learning algorithms and different modalities of data. Al-Qaness [27] improved adaptive neuro-fuzzy inference system methodology, which is based on enhanced flower pollination algorithm and slap swarm algorithm. Speech/sound analysis is conducted using computational paralinguistic [28]. Rao and Vazquez [29] proposed a method to detect COVID-19 patients using a mobile phone. However, the challenges in sound/speech technique include automatic recognition of coughing, breathing difficulties, and sneezing.

The early overview reveals different techniques for the diagnosis of COVID-19. However, the drawbacks of such techniques include patient diagnosis only after the emergence of symptoms, leading to virus spread and minimal control conditions. Additionally, none of the techniques can evaluate the necessary patient care without a doctor's intervention via required checks, which increases the burden on doctors and also possible infection with the virus due to direct contact with the patients. This work aims to provide a solution for such problems by improving the current AI techniques. This work is a part of our research in different topics and engineering solving problems, you may see the early research [30-76].

2. Diagnosis and clinical classification of COVID-19

COVID-19 is a novel virus targeting pulmonary alveoli. In critical health conditions, the infection may cause damage in the lungs and severe respiratory failure. Whenever possible, early diagnosis, isolation, and treatment of infected persons should be conducted to avoid severe or critical cases. The health condition of patients with COVID-19 can be classified into the following four cases: (a) mild cases, wherein symptoms are mild and no pneumonia manifestations are found in the lungs; (b) moderate cases, wherein symptoms, such as fever and respiratory tract symptoms, and pneumonia manifestations, can be seen in lung images; (c) severe cases, wherein the respiratory rate is larger than 30 breaths per min and oxygen saturation is less than 93% at a rest condition; additionally, the arterial partial pressure of oxygen (PaO2) is less than 300 mmHg with 50% lesion progression in the lungs [77]; and (d) critical cases, wherein the condition is more severe than the previous case (case C). Critical cases may be further divided into the following three sub-cases: (d1) early stage, (d2) middle stage, and (d3) late stage.

3. Design algorithm and representation

Different sensors are selected to read physiological indicators and electrical bio-signals. The signals are then sent into a microcontroller, which is programmed with an artificial fuzzy algorithm, to relate the acquired data with human health and take the corresponding decisions (e.g., recommendations based on human health state and level of medical care). The working principle is depicted in the flowchart as shown in Figure 1(a), and the block diagram is shown in Figure 1(b).

4. System configuration and hardware design

System structure and configuration could be proposed in different choices to read the bio-signals and physiological indicators. One option is a system design as a wearable device on top of the human head with sensors placed on head and temple sides, as shown in Figure 2. Another design option is that the system can be divided into two connected parts: one part is worn around the hand wrist, and the other part is placed on the head temple side. Some hardware components are required as follows to design the proposed system physically. Different sensors, physical control units, interfaces, communications, and power supply are applied. Synergistic integration with embedded system design methodology is applied in the system design and building processes. The hardware components are selected in small sizes (up to 5 V_{DC} operating voltage) and output signals compatible with the microcontroller ranging from 0 V_{DC} to 5 V_{DC}. Necessary hardware for reading EEG and EMG bio-signals are selected with ready-made signal processing units.

Different sensors are applied to measure bio-signals and physiological indicators of humans considering body temperature, oxygen saturation level, and heart pulse rates. Additionally, human electrical bio-signals considering signals acquired from muscle EMG and brain EEG are applied. The DS18B20 temperature waterproof sensor shown in Figure 3(a), which has a simple one-wire interface, is chosen for measuring the human body temperature. An optical heart rate sensor, which is suitable for reading heartbeats, is applied as shown in Figure 3(b). Figure 3(c) shows a maxim integrated MAX30102 high-sensitivity pulse oximeter, which is chosen to read the amount of oxygen saturation level (SpO2) in the blood. The heart rate sensor is chosen for measuring heart rate and SpO2.

The EMG and EEG signals are chosen to be in small microvolt-sized value (usually between 1 µV and 100 mV). These signals are considerably weak with noise; thus, these signals should be read, processed, and handled correctly considering amplification, filtration, and illustration. Different options to read and process the generated human brain electrical EEG bio-signal are available. However, the most suitable, simple, and easy way is to modify the light-weighted MindFlex headset, as shown in Figure 3(d). An EEG signal processing circuit is then applied as shown in Figure 3(e). However, electrical EMG impulse signals are applied to read and process the generated signals by muscle fibers. The miniaturized (suitable for wearable design) MyoWare module (AT-04-001) with the surface EMG sensor/electrode is selected as shown in Figure 3(f).

The output units needed for the system development, including LCD for data demonstration, soft light (red/green), and sound notification alarm, are applied as shown in Figure 4(a). Figure 4(b) shows the bioindicator values and the related medical care needed, which are considered on the basis of human health condition (either in positive or negative results) to display the decision taken by the artificial fuzzy algorithm. The decision shows the intensive care needed and/or resuscitation via a 4 × 20 LCD character module. The drive circuit diagram for interfacing and controlling the two alarms of the microcontroller is shown in Figure 4(c). The circuit, which comprises a z pull-down 4.7-ohm resistor, a PN222 transistor, and a 330 Ohms resistor for LED protection, is developed. A suitable microcontroller-based control unit of ATmega328p microcontroller is utilized in an Arduino Nano board, as shown in Figure 5(a). A suitable power supply of a rechargeable lithium-polymer battery type with 3.7 V and 180 mAH is chosen, as shown in Figure 5(b). Finally, batteries in parallel and series connections/combinations are applied to achieve the needed power level.

5. Overall system and subsystem design and prototyping

The complete block diagram and pictorial representation of the overall system hardware design and integration are respectively shown in Figures 6(a) and (b). All selected sensors for reading physiological indicators, mainly body temperature, pulse rate, and breathing rate/oxygen level, are interfaced to the microcontroller analog and digital pins. Additionally, the two corresponding modules are interfaced to the microcontroller-based control unit to read human electrical bio-signals considering EEG and EMG. The artificial fuzzy control algorithm (designed to read physiological indicators and bio-signal) converts signals into specific ranges of medical practice to be suitable for interpretation and relation to the human health state. These ranges are used to develop the input and output membership functions, which are discussed in fuzzy logic algorithms with further processing values, interpretation, and decision making.

The design includes human bio-signals and physiological indicators to assess health conditions of body temperature, heart pulse rate, SPO2 level, and EMG and EEG signals. These bio-signals and indicators, in conjunction with other criteria, serve as early detection systems for determining the health conditions of any person with COVID-19 infection and identifying necessary further assessment and/or treatment. The normal values of vital human signs and units are summarized in Table 1.

The DS18B20 measures human skin temperature, and this measured value is used to estimate human body temperature; based on standards, the rough skin temperature is approximately 5.1 °C lower than body temperature [78]. The DS18B20 temperature sensor is interfaced with the microcontroller through 4.7 K Ohms resistor and a wire signal of 5 V. Software integration with a manufacturer programming library is used to read the generated temperature signal and then calculate the body temperature in Celsius degrees. The initial step in a full clinical examination is reading the human body temperature. Medical reports indicate that this body temperature slightly varies depending on age, time of day, and activity. The human body temperature is divided into different ranges and corresponding interpretations. Normal body temperature is considered within the range from 36.1 °C to 37.5 °C. A body temperature between 37.7 °C to 38.3 °C often indicates hyperthermia and fever caused by an illness or an infection, and that between 38.3 °C to 40.0 °C indicates a high fever. A body temperature higher than 40 °C/41.5 °C indicates hyperpyrexia with dinger fever and body risk. By contrast, a body temperature of less than 35.0 °C indicates hypothermia (low temperature).

The amount of arterial oxygen saturation level in the blood, shortly named SpO2, is a useful tool used to evaluate the severity of an illness. SpO2 level is recommended for the early detection of COVID-19 pneumonia, which infects human lungs, resulting in inflammation and pneumonia. The affected negatively on oxygen transferred from the lungs into the bloodstream. Clinically, a substantially low oxygen level is observed in a patient infected with COVID-19 despite normal appearance. By contrast, clarifying that some patients with COVID-19 are not suffering from low oxygen level is important. The arterial levels of SpO2 are divided into the following ranges and corresponding interpretations: normal and healthy arterial level (SpO2 within 95%–100%), mild hypoxemia (SpO2 within 91%–94%), hypoxic (arterial level of SpO2 is within 85%–94%), and severely hypoxic (arterial level of SpO2 below 85%). An outbreak due to COVID-19 is generally considered at SpO2 below 90%; in such a case, a medical re-evaluation is highly recommended.

Heart rate, also called pulse rate, is the number of beats per minute for the human heart. One heart rate is different from the blood pressure, which is the blood force against the walls of blood vessels. Infection of COVID-19 is associated with variations in heart rate with fluctuating pulse rate, which generally increases with illness, injury, exercise, and emotions. The health condition of a person infected with COVID-19 is associated with an increase in heart rate; therefore, heart rate parameter helps detect COVID-19 [79]. The heart rate for adult's ranges between 60 and 100 beats per min for a normal resting condition. A high heart rate (above 100 bpm) could be an indication of COVID-19 infection symptom. Maxim integrated type MAX30102 with a high-sensitivity pulse oximeter is a heart-rate sensor used to read heart rate and SpO2. In such a sensor, only four pins are used with SDA and SCL wired to the microcontroller analog pins. Software integration with manufacturer programming libraries is used to read the two signals and then interpret their values.

Respiratory rate, also called breathing rate, is the number of breaths (inhalation and exhalation) per minute (bpm). In the case of COVID-19 infection, the respiratory rate of a person is increased while experiencing significant or sudden shortness of breath and other health troubles. The normal respiratory rate at rest of an adult is between 12 to 16 bpm. Values outside this range are considered abnormal. Tachypnea indicates that the respiratory rate is larger than 20 bpm. For the elderly older than 65 years old, the normal respiratory rate is between 12 and 28 bpm, which should be considered for sensor readings.

EEG reads brain electrical activity from the human scalp considering microvolt signals using electrodes, while EMG reads electrical impulses generated by muscle fibers. Viral infection can cause muscle pain and relaxation, including facial muscles. Muscle pain can also be due to exercise. Thus, distinguishing between pain from COVID-19 and other causes is difficult. A detailed analysis indicates that pains caused by COVID-19 are often incapacitating, sharp, and persistent for around a couple of weeks. Additionally, COVID-19-related muscular symptoms include myalgia (tiredness and muscle pain/aches) and headache, and such symptoms can be read and interpreted from EMG and EEG. The EEG and EMG signals are applied in this work to detect health conditions, such as myalgia, dizziness, headache, and sleeping problems. These data are then related to predicting and diagnosing COVID-19 infection. The light-weighted MindFlex headset shown in Figure 3(d) is a single EEG channel device used to read electrical activities of the human brain.

Figure 3(f) shows the MyoWare module EMG, which is a ready-made module for reading, filtering, and rectifying the electrical impulses generated by muscle fibers via EMG electrodes. The sensor output voltage is proportional to the selected muscle activities [80]. Software integration is applied for the reading ranges between 0 and 5 VDC according to muscle activity.

A fuzzy algorithm model is developed to evaluate the human health condition. Consequently, this model is used to estimate the probability of COVID-19 infected person(s) based on reading human vital sign indicators and the changes in their values. The fuzzy algorithm applied bio-signals and physiological indicators of humans as input values. The base knowledge and inference mechanisms are designed to relate such values and take the decision regarding human COVID-19 infection via four previously discussed different cases: *(a)* mild, (b) moderate, (c) severe, and (d) critical cases. The fuzzy logic algorithm is designed and established in MATLAB/Simulink approach. Five input membership functions are developed using five input bio-signals and indicators as shown in Figure 7: body temperature, pulse (heart) rate, SPO2 level, EMG, and EEG; additionally, one output membership function is considered. The linguistic variables for each membership function and its corresponding ranges are designed following established ranges. The interpretation and indications are summarized in Table 2.

6. Testing, evaluation, and discussions

All subsystems, components, and hardware issues are tested in different scenarios. Additionally, the overall system design is tested and validated as explained subsequently. The microcontroller/Arduino with Excel communication is established to test the operation, reading, and software integration of each sensor to read the data from sensors and then save the results in an Excel file. Afterward, such data are analyzed for a health evaluation, and the data are displayed. The readings and display of data from all sensors for one test case are shown in Figure 8 as an example. The testing results of all sensors are successfully acquired, saved, and represented in numerical and graphical forms. Only these readings can be used by specialists for analyzing and relating the values; they can also define the health condition and distinguish between healthy and infected person(s).

The artificial fuzzy algorithm, applying the knowledge base rule and interference mechanism, interprets and relates the input values of each/all five bio-signals and physiological indicators; then the evaluation condition and the health state take place with the proper decision about person condition in terms of clinical classification of COVID-19 infection (discussed early). These cases are then used to report the level of medical care needed considering intensive care and/or resuscitation. The COVID-19 classification cases, fuzzy decision, numerical values, medical care needed, and color visualization on the patient condition are all listed in Table 3.

Testing the overall system designs is accomplished in the current study by integrating all subsystems and components into one overall system, as shown in Figure 6(b). The hardware in-loop simulation using the input hardware sensors, Arduino board, and laptop with MATLAB/Simulink are all integrated into one overall system model, as shown in Figure 9. Two scenarios are applied to test the system design and vary (increasing and decreasing) the bio-signals and physiological indicators of a given person. The first scenario aims to examine warming-up and relaxing physical exercises, such as pushups, run around, and meditation. The second scenario is applied in a real case with a person who got a cold infection. The results of the two examples are evaluated considering input values of bio-signals and physiological indicators and the results with the final decision taken of medical care needed.

7. Conclusions

This work develops AI techniques for the diagnosis of COVID-19 symptoms in a considerably fast time with high accuracy and overcomes some issues of the available AI. The work covers simulation, hardware design, and validation of a sophisticated AI diagnosis system. The system utilized an artificial fuzzy inelegance for determining a patient's health condition with COVID-19 and distinguishing between other close symptoms and COVID-19 infected persons. Moreover, the system provides a report containing the health condition and the level of medical care needed without any human intervention in a considerably fast time (seconds), which allows the examination of numerous people in a substantially short time without running cost. The system measures many vital biological and human functions and, then analyzes the data and issues a detailed report on the health condition. Hardware designs are applied to select suitable components for the system and software incorporation. The experimental study is applied to examine and test the proposed system. The results showed that the proposed system could be used to distinguish between healthy and infected individuals before the onset of COVID-19 symptoms.

Acknowledgment

Authors would like to acknowledge the financial support received from the Scientific Research Deanship, Taif University, KSA, through grant number 1– 441– 42.

Conflict of Interest

There are no conflicts of interest in this study.

References

[1]. N. Zhu, D. Zhang, W. Wang, A Novel Coronavirus from Patients with Pneumonia in China, 2019. N Engl J Med. 2020 Jan 24. doi: 10.1056/NEJMoa2001017.

[2]. Q. Li, X. Guan, P. Wu, Early Transmission Dynamics in Wuhan, China, of Novel Coronavirus-Infected Pneumonia, J. N Engl J Med. 2020 Jan 29. doi: 10.1056/NEJMoa2001316.

[3]. J. Cohen, D. Normile, New SARS-like virus in China triggers alarm, J. Science. 2020 Jan 17; 367(6475):234-235. doi: 10.1126/science.367.6475.234.

[4]. V. M. Corman, O. Landt, M. Kaiser, Detection of 2019 novel coronavirus (2019-nCoV) by real-time RT-PCR. Euro Surveill. 2020 Jan; 25(3). doi: 10.2807/1560-7917.ES.2020.25.3.2000045.

[5]. C. Huang, Y. Wang, X. Li, Clinical features of patients infected with 2019 novel coronavirus in Wuhan, China, Lancet. 2020 Jan 24. pii: S0140-6736(20)30183-5. doi:10.1016/S0140-6736(20)30183-5.

[6]. D. Wang, B. Hu, C. Hu, F. Zhu, X. Liu, J. Zhang, et al., "Clinical characteristics of 138 hospitalized patients with 2019 novel coronavirus–infected pneumonia in Wuhan, China, " Jama, 2020.

[7]. N. Chen, M. Zhou, X. Dong, J. Qu, F. Gong, Y. Han, et al., "Epidemiological and clinical characteristics of 99 cases of 2019 novel coronavirus pneumonia in Wuhan, China: a descriptive study, " The Lancet, vol. 395, pp. 507-513, 2020.

[8]. O. Gozes, M. Frid-Adar, H. Greenspan, P. D. Browning, H. Zhang, W. Ji, A. Bernheim, E. Siegel, Rapid AI Development Cycle for the Coronavirus (COVID-19) Pandemic: Initial Results for Automated Detection & Patient Monitoring using Deep Learning CT Image Analysis, arXiv preprint arXiv:2003.05037, 1-19, 2020.

[9]. X. Liu, S. Guo, B. Yang, Automatic Organ Segmentation for CT Scans Based on Super-Pixel and Convolutional Neural Networks, Journal of Digital Imaging, 2018, 31(6). 26 / 29

[10]. M. Gharbi, J. Chen, J. T. Barron, Deep Bilateral Learning for Real-Time Image Enhancement, J. Acm Transactions on Graphics, 2017, 36(4):118.

[11]. M. H. Hesamian, W. Jia, X. He, Deep Learning Techniques for Medical Image Segmentation: Achievements and Challenges, Journal of Digital Imaging, 2019, 32(8).

[12]. M. Akagi, Y. Nakamura, T. Higaki, Correction to: Deep learning reconstruction improves image quality of abdominal ultra-high-resolution CT, J. European Radiology, 2019, 29(8).

[13]. P. Nardelli, D. Jimenez-Carretero, D. Bermejo-Pelaez, Pulmonary Artery-Vein Classification in CT Images Using Deep Learning, J. IEEE Transactions on Medical Imaging, 2018, PP (99):1-1.

[14]. W. Zhu, Y. Huang, L. Zeng, Anatomy Net: Deep learning for fast and fully automated whole-volume segmentation of head and neck anatomy, J. Medical Physics, 2019, 46(2).

[15]. F. Shan, Y. Gao, J. Wang, W. Shi, N. Shi, M. Han, Z. Xue, Y. Shi, Lung Infection Quantification of COVID-19 in CT Images with Deep Learning, arXiv preprint arXiv:2003.04655, 1-19, 2020.

[16]. X. Xu, X. Jiang, C. Ma, P. Du, X. Li, S. Lv, L. Yu, Y. Chen, J. Su, G. Lang, Y. Li, H. Zhao, K. Xu, L. Ruan, W. Wu, Deep Learning System to Screen Coronavirus Disease 2019 Pneumonia, arXiv preprint arXiv:2002.09334, 1-29, 2020.

[17]. S. Wang, B. Kang, J. Ma, X. Zeng, M. Xiao, J. Guo, M. Cai, J. Yang, Y. Li, X. Meng, B. Xu, A deep learning algorithm using CT images to screen for Corona Virus Disease (COVID-19). medRxiv preprint doi: https://doi.org/10.1101/2020.02.14.20023028, 1-26, 2020

[18]. A. Hamimi, MERS-CoV: Middle East respiratory syndrome corona virus: Can radiology be of help? Initial single center experience. The Egyptian Journal of Radiology and Nuclear Medicine, 47(1): 95-106, 2016.

[19]. C. Szegedy, W. Liu, Y. Jia, P. Sermanet, S. Reed, D. Anguelov, D. Erhan, V. Vanhoucke, A. Rabinovich, Going deeper with convolutions, In Proceedings of the IEEE conference on computer vision and pattern recognition, pp. 1–9, 2015.

[20]. Z. Zhou, M. M. R. Siddiquee, N. Tajbakhsh, J.

Liang, Unet: A nested u-net architecture for medical image segmentation, In Deep Learning in Medical Image Analysis and Multimodal Learning for Clinical Decision Support, pp. 3–11. Springer, 2018.

[21]. J. Chen, L. Wu, J. Zhang, L. Zhang, D. Gong, Y. Zhao, S. Hu, Y. Wang, X. Hu, B. Zheng, Deep learning-based model for detecting 2019 novel coronavirus pneumonia on high-resolution computed tomography: a prospective study. medRxiv preprint medRxiv:2020.02.25.20021568, 2020.

[22]. A. w. Linda Wang, "COVID-Net: A Tailored Deep Convolutional Neural Network Design for Detection of COVID-19 Cases from Chest Radiography Images," 2020.

[23]. S. Wang, B. Kang, J. Ma, X. Zeng, M. Xiao, J. Guo, M. Cai, J. Yang, Y. Li, X. Meng, B. Xu, A deep learning algorithm using CT images to screen for Corona Virus Disease (COVID-19), doi: https://doi.org/10.1101/2020.02.14.20023028; February 17, 2020, p. 2020.02.14.20023028, 2020.

[24]. A. S. Joaquin. Using Deep Learning to detect Pneumonia caused by NCOV-19 from X-Ray Images. Available: https://towardsdatascience.com/using-deep-learning-to-detectncov-19-from-x-ray-images-1a89701d1acd, 2020.

[25]. L. Yan, H.-T. Zhang, Y. Xiao, M.Wang, C. Sun, J. Liang, S. Li, M. Zhang, Y. Guo, Y. Xiao et al., "Prediction of criticality in patients with severe covid-19 infection using three clinical features: a machine learning-based prognostic model with clinical data in wuhan," medRxiv, 2020.

[26]. K. Santosh, "Ai-driven tools for coronavirus outbreak: Need of active learning and cross-population train/test models on multitudinal/multimodal data," Journal of Medical Systems, vol. 44, no. 5, pp. 1–5, 2020.

[27]. M. A. Al-Qaness, A. A. Ewees, H. Fan, and M. Abd El Aziz, "Optimization method for forecasting confirmed cases of covid-19 in china," Journal of Clinical Medicine, vol. 9, no. 3, p. 674, 2020.

[28]. B. Schuller and A. Batliner, Computational Paralinguistics: Emotion, Affect and Personality in Speech and Language Processing. Wiley, 2013.

[29]. A. S. S. Rao and J. A. Vazquez, "Identification of covid-19 can be quicker through artificial intelligence framework using a mobile phonebased survey in the populations when cities/towns are under quarantine,"Infection Control & Hospital Epidemiology, pp. 1–18, 2020.

[30]. A. Elfasakhany, X.S. Bai, "Simulation of Wood Powder Flames in a Vertical Furnace" *3rd Medit. Combustion Symposium*, Marrakech, p. 144, 2003.

[31]. A. Elfasakhany, X.S. Bai**,** B. Espenas, L. Tao, J. Larfeldt, "Effect of Moisture and Volatile Releases on Motion of Pulverised Wood Particles*", 7th Int. Conf. on Energy for a Clean Environment*, Lisbon, Portugal, p. 167, 2003.

[32]. A. Elfasakhany "Modeling of Pulverised Wood Flames", PhD Thesis*,* fluid mechanics dept., Lund, Sweden, *ISBN-13/EAN:* ***9789162864255,*** 2005.

[33]. A. Elfasakhany, X.S. Bai, "Modeling of Pulverised Wood Combustion: A Comparison of Different Models", *Prog. Comp. Fluid Dynamics (PCFD), Scopus, ISI* , Vol. 6, No. 4/5, p. 188–199, 2006.

[34]. A. Elfasakhany, T. Klason ,X.S. Bai, "Modeling of Pulverised Wood Combustion Using a Functional Group Model", *Combustion Theory and Modeling*, *Scopus, ISI* , Vol. 12, 5, 883–904, 2008.

[35]. A. Elfasakhany, E.Y. Rezola, K.B. Quiñones, R.S. Sánc, "Design and Development of a Competitive Low-cost Robot Arm with Four Degrees of Freedom", *Modern Mechanical Eng,* vol. 1, 47–55, 2011.

[36]. A. Elfasakhany, J. Hernández, J. C. García, M. Reyes, F. Martell, "Design and Development of House-Mobile Security System", Engineering, vol. 3, 1213–1224, 2011.

[37]. A. Elfasakhany, A. Arrieta, D. M. Ramírez, F. Rodríguez, "Design and Development of an Autonomous Trash Sorting System". *Global J. of Pure and Applied Sciences and Tech.*, vol. 01i3, 56–64, 2011.

[38]. A. Elfasakhany, L. Tao, B. Espenas, J. Larfeldt, X.S. Bai "Pulverised Wood Combustion in a Vertical Furnace: Experimental and Computational Analyses" International Conference of Applied Energy, 2012.

[39]. A. Elfasakhany, J. Marquez, E.Y. Rezola, J. Benitez "Design and Development of an Economic Autonomous Beverage Cans Crusher" *Int. J. of Mech. Eng. Tech.* Vol. 3, Issue 3, 107–122, 2012.

[40]. A. Elfasakhany "Improving Performance and Development of Two-Stage Reciprocating Compressors" *Int. J. of Advanced Research in Eng. Tech.* Vol. 3, Issue 2, 119–136, 2012.

[41]. A. Elfasakhany "Modeling of Secondary

Reactions of Tar (SRT) Using a Functional Group Model" *Int. J. of Mech. Eng. Tech.* Vol. 3, Issue 3, 123–136, 2012.
[42]. A. Elfasakhany, J. A. Alarcón, D. O. S. Montes " Design and Development of an Automotive Vertical Doors Opening System (AVDOS)" *Int. J. of Advanced Research in Eng. Tech.* Vol. 3, 176–186, 2012.
[43]. A. Elfasakhany, Jaime Luis Jiménez, Iván Arturo Rentería, Juan Manuel Rubio, Wilians Damian Ricardez "Design, Development, Testing and Validation of an Automower Machine" *Int. J. of Applied Mechanics and Physics,* Vol. 1, No. 1, 1–15, 2013.
[44]. A. Elfasakhany "Investigation on performance and emissions characteristics of an internal combustion engine fuelled with petroleum gasoline and a hybrid methanol–gasoline fuel" *Int. J. of Eng. Tech. (IJET-IJENS)* Vol.13 No:05, 24–43, 2013.
[45]. A. Elfasakhany, L. Tao, B. Espenas, J. Larfeldt, X.S. Bai "Pulverised Wood Combustion in a Vertical Furnace: Experimental and Computational Analyses" *Applied Energy*, *Elsevier,* Vol. 112, 454–464, 2013.
[46]. A. Elfasakhany "Experimental study on emissions and performance of an internal combustion engine fueled with gasoline and gasoline/n-butanol blends" *Energy Conversion Manage, Elsevier,* Vol. 88, 277–283, 2014.
[47]. A. Elfasakhany, L.X. Tao, X.S. Bai "Transport of pulverized wood particles in turbulent flow: numerical and experimental studies" *Energy Procedia*, *Elsevier,* Vol. 61, 1540–1543, 2014.
[48]. A. Elfasakhany "Experimental investigation on SI engine using gasoline and a hybrid iso-butanol/gasoline fuel" *Energy Conversion and Management*, *Elsevier,* Vol. 95, 398–405, 2015.
[49]. A. Elfasakhany "Investigations on the effects of ethanol-methanol-gasoline blends in a spark-ignition engine: performance and emissions analysis" *Engineering Science Technology, Elsevier,* Vol. 18, 713–719, 2015.
[50]. A. Elfasakhany "Experimental study of dual n-butanol and iso-butanol additives on spark-ignition engine performance and emissions" *Fuel*, *Elsevier,* Vol. 163, 166–174, 2016.
[51]. A. Elfasakhany "Performance and emissions analysis on using acetone–gasoline fuel blends in spark ignition engine" *Engineering Science Technology, Elsevier,* Vol. 19, 1224–1232, 2016.
[52]. A. Elfasakhany, A.-F. Mahrous "Performance and emissions assessment of n-butanol–methanol–gasoline blends as a fuel in spark-ignition engines" *Alexandria Engineering J., Elsevier*, Vol. 55, 3015–3024, 2016.
[53]. A. Elfasakhany "Performance assessment and productivity of a simple-type solar still integrated with nanocomposite energy storage system" *Applied Energy*, *Elsevier,* Vol. 183, 399–407, 2016.
[54]. A. Elfasakhany "Engine performance evaluation and pollutant emissions analysis using ternary bio-ethanol–iso-butanol–gasoline blends in gasoline engines" *Cleaner Production*, *Elsevier,* Vol. 139, 1057–1067, 2016.
[55]. A. Elfasakhany "Performance and emissions of spark-ignition engine using ethanol–methanol–gasoline, n-butanol–iso-butanol–gasoline and iso-butanol–ethanol–gasoline blends: a comparative study" *Engineering Science Technology, Elsevier,* Vol. 19, 2053–2059, 2016.
[56]. A. Elfasakhany "Investigations on performance and pollutant emissions of spark-ignition engines fueled with n-butanol–, iso-butanol–, ethanol–, methanol–, and acetone–gasoline blends: a comparative study" *Renewable & Sustainable Energy Reviews*, *Elsevier* , Vol. 71, 404–413, 2017.
[57]. A. Elfasakhany " Design, analysis and optimization of the tail bearing housing of jet engine" J. Advances in Vehicle Engineering, Canada, *Scopus, ISI* , Vol. 3, 99–111. 2017.
[58]. A. Elfasakhany " Exhaust emissions and performance of ternary iso-butanol–bio-methanol–gasoline and n-butanol–bio-ethanol–gasoline fuel blends in spark-ignition engines: assessment and comparison" Energy, *Elsevier,* Vol. 158, 830–844, 2018.
[59]. A. Elfasakhany, "Powder biomass fast pyrolysis as in combustion conditions: Numerical prediction and validation", *Renewable Energy Focus*, *Elsevier,* Vol. 27, 78-87, 2018.
[60]. A. Elfasakhany "A New Patent of Beverage Cans Crusher Machine" *Current Alternative Energy*, Vol. 2, Issue 2, 123–131, *2018.*
[61]. A. Elfasakhany "Beverage Cans Crusher Machine Patents: A Review: Part I" *Asian Review of Mechanical Engineering*, Vol.7, No. 2, 62–69, 2018.
[62]. A. Elfasakhany "Beverage Cans Crusher Machine Patents: A Review (Part II)" *Asian Review of Mechanical Engineering*, Vol.7, No. 2, 76–82, 2018.

[63]. A. Elfasakhany "Biofuels in Automobiles: Advantages and Disadvantages: A Review" *Current Alternative Energy*, Vol. 3, Issue 1, 1–7, *2019.*
[64]. A. Elfasakhany "Beverage Cans Crusher Machine Patents: A Review (Part III)" *Asian Review of Mechanical Engineering*, Vol.8, No. 1, 1–7, 2019.
[65]. A. Elfasakhany, X. S. Bai, "Numerical and experimental studies of irregular-shape biomass particle motions in turbulent flows", *Engineering Science Technology, Elsevier,* Vol. 22, 249–265, 2019.
[66]. A. Elfasakhany "Beverage Cans Crusher Machine Patents: A Review (Part IV)" *Asian Review of Mechanical Engineering*, Vol. 8, No. 1, 11–17, 2019.
[67]. A. Elfasakhany "Beverage Cans Crusher Machine Patents: A Review (Part V)" *Asian Review of Mechanical Engineering*, Vol. 8, No. 1, 31–38, 2019.
[68]. A. Elfasakhany "Tire pressure checking framework: a review study" *Reliability Engineering and Resilience*, Vol. 1, Issue 1, 12–28, 2019.
[69]. A. Elfasakhany "Beverage Cans Crusher Machine Patents: A Review: Part VI" Open Access *Journal of Environmental and Soil Sciences*, 4(3): 511–518, 2020.
[70]. A. Elfasakhany "How Evaporator of Automotive Air Conditioner is Modelled? A Systematic Review" *Applications of Modeling and Simulation (AMS),* VOL 4(1), 64–70, 2020.
[71]. Ashraf Elfasakhany, Mishal Alsehli, Bahaa Saleh, Ayman A. Aly, Mohamed Bassuoni "Renewable Pulverized Biomass Fuel for Internal Combustion Engines" Processes, ISI, Vol. 8 (4), 465, 2020.
[72]. A. Elfasakhany "Gasoline engine fueled with bioethanol-bio-acetone-gasoline blends: Performance and emissions exploration" Fuel, Elsevier, Vol. 274, 117825, 2020.
[73]. A. Elfasakhany "Beverage Cans Crusher Machine Patents: A Review: Part VII" International Journal of Research and Scientific Innovation (IJRSI), Volume VII, Issue IV, 239–247, 2020.
[74]. A. Elfasakhany "Beverage Cans Crusher Machine Patents: A Review: Part VIII" International Journal of Research and Scientific Innovation (IJRSI), Volume VII, Issue V, 6–15, 2020.
[75]. A. Elfasakhany "Alcohols as Fuels in Spark Ignition Engines: Second Blended Generation" *Germany*, ISBN: 978-3-659-97691-9, 2017.
[76]. A. Elfasakhany "Benefits and drawbacks on the use biofuels in spark ignition engines" *Mauritius*, ISBN: 978-620-2-05720-2, 2017.
[77]. Diagnosis and treatment plan of Corona Virus Disease 2019 (tentative sixth edition). Global Health Journal, March 30, 2020, Volume 4, Issue 12 Pages 1-5.
[78]. R. Lenhardt, D. I. Sessler, Estimation of mean-body temperature from mean-skin and core temperature, Anesthesiology, vol. 105, no. 6, pp. 1117–1121, Dec. 2006.
[79]. C. Baumann, R. Buchhorn, C. Willaschek, Heart Rate Variability in a Patient with Coronavirus Disease 2019, https://www.preprints. org/manuscript /202005.0209/ v1 [accesses 13/09/2020]
[80]. S. Ahmed, Intelligent Bio-Detector, Open Journal of Applied Sciences, 2016, 6, 903-937.

Tables and Figures

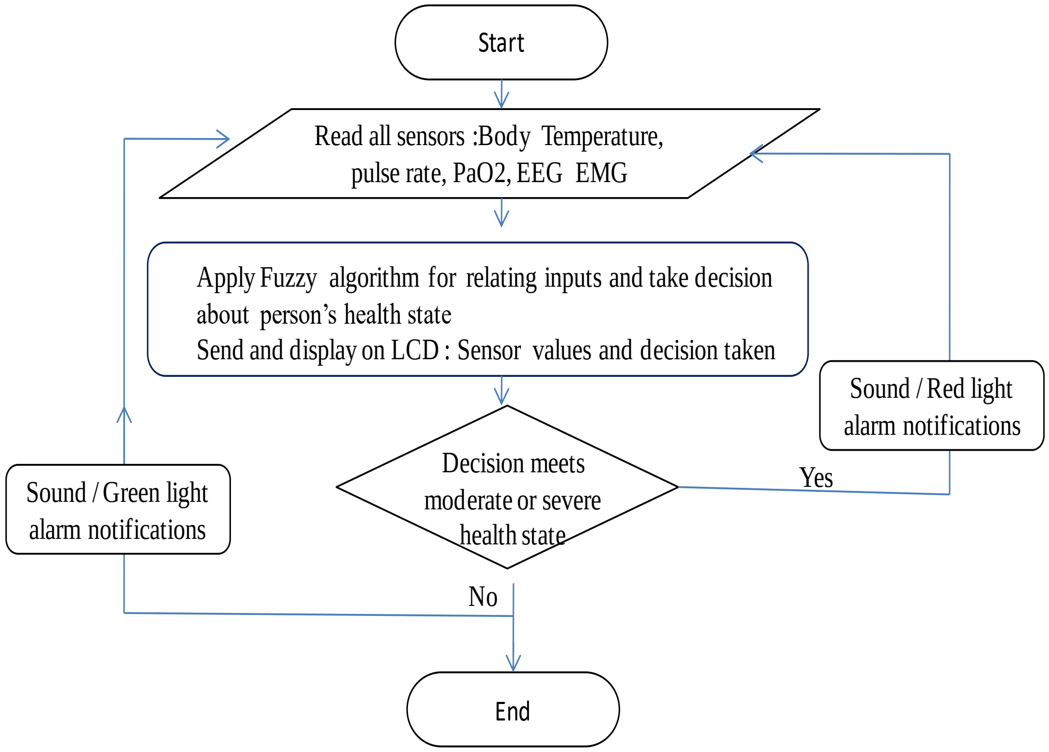

Figure 1(a). **The system working algorithm represented using flowcharts.**

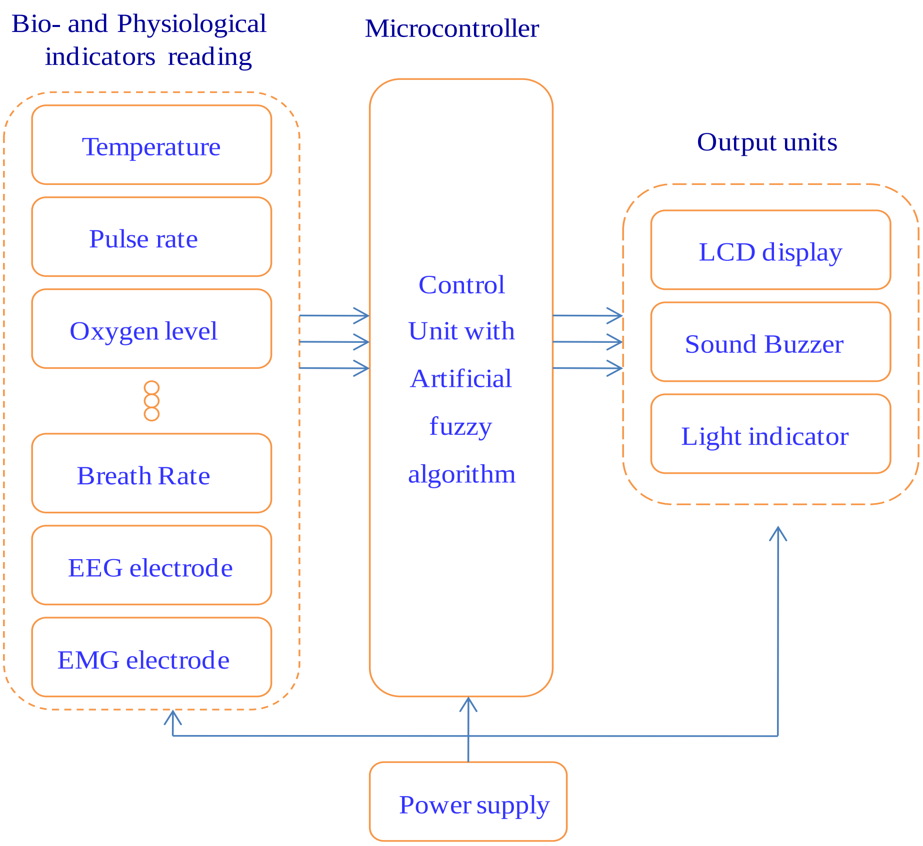

Figure 1(b). **System design representation using block diagram.**

Figure 2 suggested structure for the system with sensors placement

Figure 3(a): the DS18B20 Temperature sensor

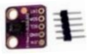

Figure 3(b): Optical heart rate sensor

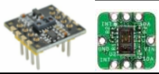

Figure 3(c): Oximeter and Heart Rate Monitor.

Figure 3(d): The mindflex headset EEG reading

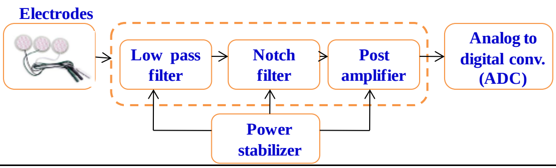

Figure 3(e): EEG signal processing circuit

Figure 3(f): MyoWare module EMG reading

Figure 4(a): LEDs and buzzer alarm.

Figure 4(b): 4x20 LCD, characters module

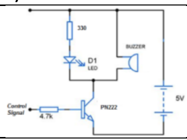

Figure 4(c): circuit diagram for interfacing alarms

Figure 5(a): ATmega328p microcontroller-based board

Figure 5(b): Li-Po li ion, 3.7V Battery

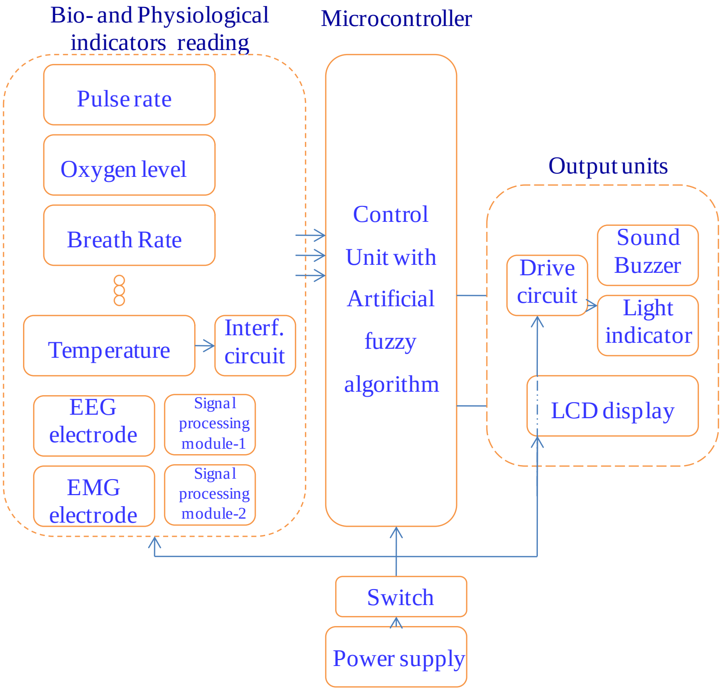

Figure 6(a). **System's detailed block diagram representation.**

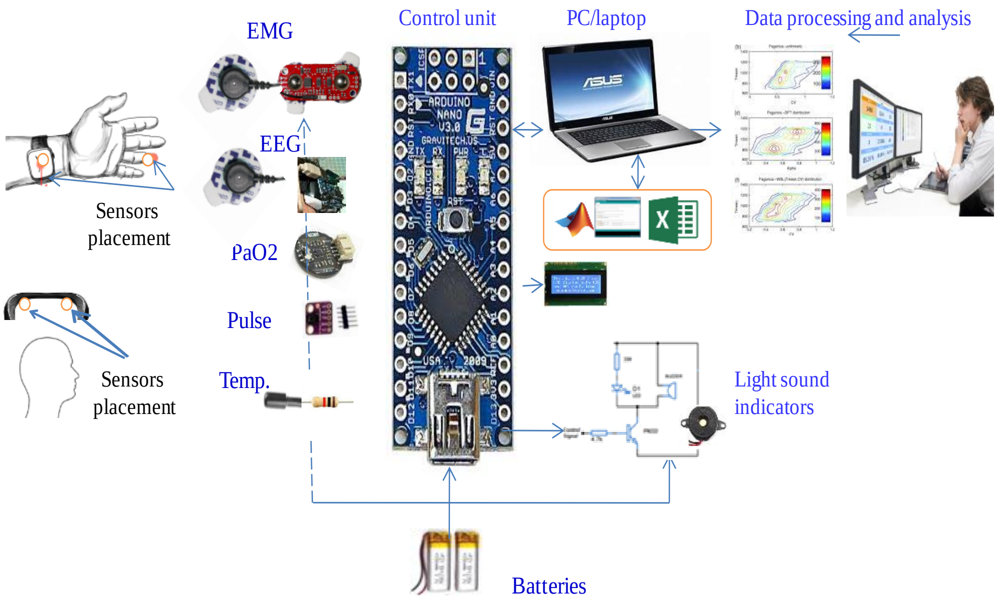

Figure 6(b). **Pictorial integrated hardware design of the suggested system.**

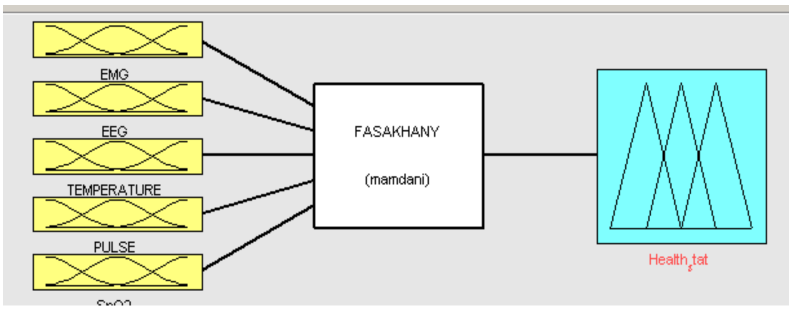

Figure 7. **Fuzzy algorithm developed in MATLAB/Simulink**

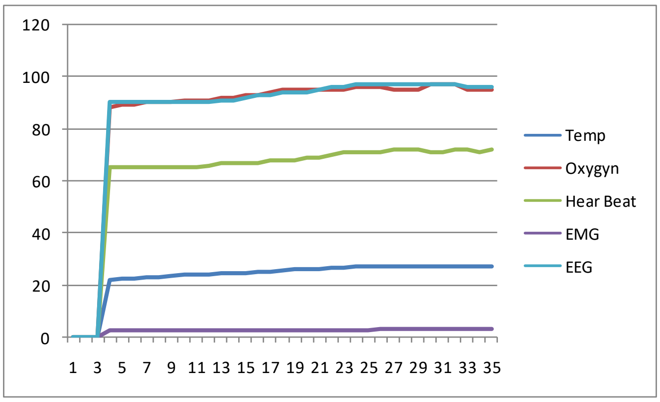

Figure 8. **An example on reading and displaying all sensors' reading values (the five bio-signals and Physiological indicators).**

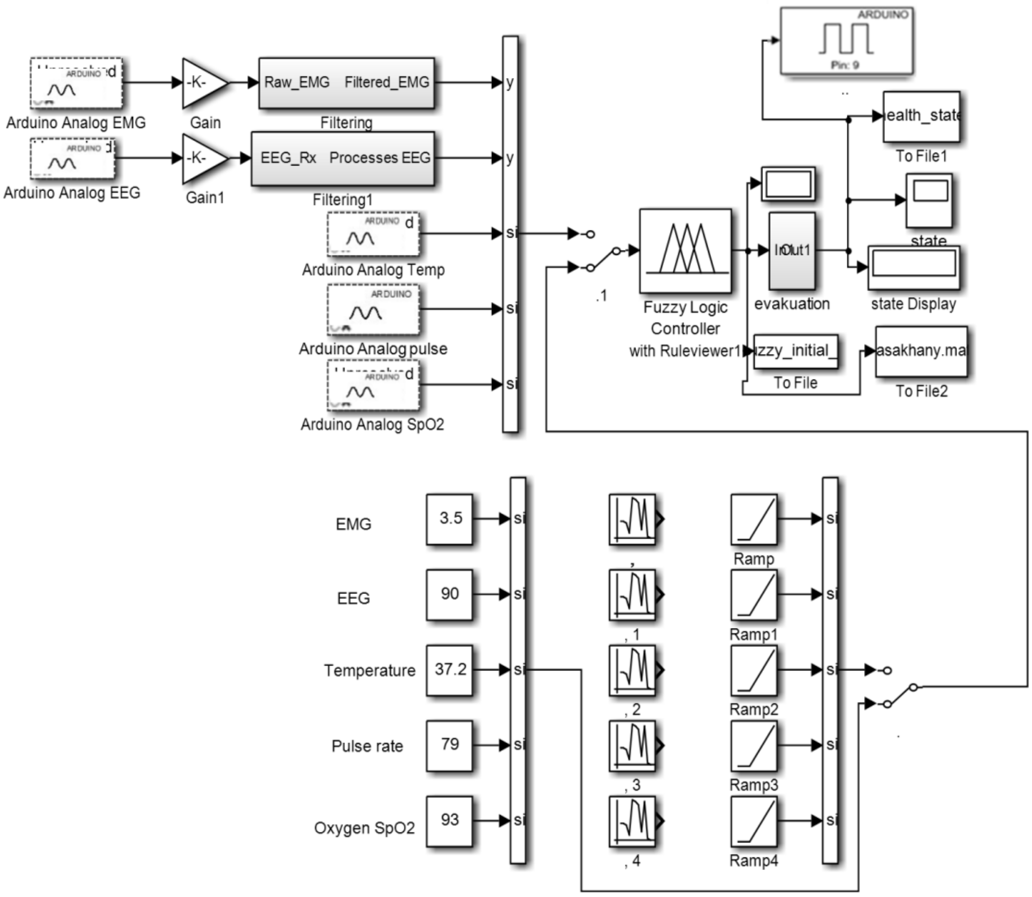

Figure 9. **Overall system design testing with the hardware in-loop simulation using the input hardware sensors, Arduino board, and Laptop with MATLAB/Simulink.**

Table 1. **Vital human signs and normal values in adults.**

Indictor	Normal value and unit
Temperature	37°C
Heart pulse Rate	60-99 bpm (beat per minute)
Oxygen saturation, SPO2	95-100%
Respiratory rate	12-16 Breaths per minutes
Blood pressure	120/80 mmHg

Table 2. **Established ranges and interpretations for the input membership functions.**

Indicator	Ranges and indications				
	less than (35.0 °C)	(36.1 °C) to (37.5 °C).	(37.7 °C) to (38.3 °C or infection.	(38.3 °C) to (40.0 °C)	Larger than (40.0 °C or 41.5 °C)
Body temperature	Indicates hypothermia (low temperature)	Indicates normal body temperature	Indicates hyperthermia), which is fever caused by an illness or an infection	Indicates high fever	Indicates hyperpyrexia, which is fever with an extreme elevation of body temperature
	(95%–100%),	(91%–94%)	less than 90%	below (85%)	_
SpO2 level	Indicates normal and healthy arterial level	Indicates mild hypoxemia, which is below-normal blood oxygen level	Indicates low oxygen level; a medical re-evaluation is highly recommended	Considered severely hypoxic for a human	_
	(60–90) beats per minute	(90–100)	Above (100 bpm)	_	_
Heart rate	Considered normal	Indicates mild sign of infection	Could be a sign of infection and indicates serious COVID-19 symptoms	_	_

Table 3. **Infection cases, fuzzy decision numerical value, and color applied.**

Fuzzy decision numerical value	**COVID-19 infection state**	**Health state**	**Color**	medical care needed
Between 0: 2	not infected	Good	Green	No care needed
Between 2: 4	Mild Case	Caution	Red	hypnosis
Between 4: 6	Moderate Case	high Caution	Red	intensive care, (ICU)
Between 6: 8	Severe Case/ Critical Cases	Danger	Red	Resuscitation